Crystal Structure of the Complex between Prokaryotic Ubiquitin-like Protein and Its Ligase PafA

Crystal structure of the complex between Prokaryotic Ubiquitin-like Protein Pup and its Ligase PafA

Jonas Barandun, Cyrille L. Delley, Nenad Ban and Eilika Weber-Ban*

ETH Zurich, Institute for Molecular Biology & Biophysics, CH-8093 Zurich, Switzerland

Supporting Information

ABSTRACT: Prokaryotic ubiquitin-like protein Pup is covalently attached to target proteins by the ligase PafA, tagging substrates for proteasomal degradation. The crystal structure of Pup in complex with PafA, reported here, reveals that a long groove wrapping around the enzyme serves as a docking site for Pup. Upon binding, the C-terminal region of the intrinsically disordered Pup becomes ordered to form two helices connected by a linker, positioning the C-terminal glutamate in the active site of PafA.

Pupylation is a ubiquitin-like post-translational modification in actinobacteria involving the covalent attachment of a 60-70 amino acid polypeptide termed Pup (prokaryotic ubiquitin-like protein) to a target substrate[1-6], thereby marking it for proteasomal degradation[2-4,7]. In *Mycobacterium tuberculosis* (*Mtb*) the Pup-proteasome system contributes to pathogenicity by supporting its persistence inside the host[8,9].

Despite the functional analogy to ubiquitination, the components of the pupylation pathway are not homologous to their counterparts in the ubiquitination pathway[1,6]. Unlike the stable β-grasp fold of Ub[10], Pup is an intrinsically disordered protein with only very weak propensity for helical secondary structure in its C-terminal half[11-13]. On the sequence level, the only common feature is a di-glycine motif at the C-terminal end, which in case of Ub constitutes the last two residues while in Pup it is followed by a glutamate or glutamine as the C-terminal residue. Both modifiers are coupled to the target protein through their C-terminal amino acid[1,6]. In contrast to ubiquitination, which employs a cascade of enzymes[14], pupylation is carried out by a single ligase, the Pup ligase PafA (proteasome accessory factor A)[4,5]. This enzyme, evolutionarily related to glutamine synthetases[15], turns over ATP generating a γ-glutamyl-phosphate Pup intermediate poised for the nucleophilic attack of a substrate lysine side chain to form the isopeptide bond[5,16,17]. In mycobacteria and other actinobacteria, Pup is encoded with a C-terminal glutamine (PupQ), necessitating deamidation of the C-terminal side chain by Dop (deamidase of Pup)[5], a homolog of PafA, to produce the carboxylate-group involved in the ligation (PupE). In addition, the PafA homolog Dop catalyzes the specific cleavage of the isopeptide bond between Pup and target substrates[18,19]. Pupylated proteins are recognized by the proteasomal ATPase ARC (Mpa in *Mtb*) that unfolds them and translocates them into the proteasome degradation chamber[3,4,7,13,20]. The N-terminal coiled-coil domains of the ATPase bind Pup, which forms an elongated helix upon complex formation (residue 21-51 of Pup_{Mtb})[13,20].

We previously reported structures of Dop and PafA in absence of Pup[21]. Both enzymes feature a large N-terminal domain (~400 residues) homologous to glutamine synthetases and a small C-terminal domain (~70 residues) unique to Dop and PafA. Nuclear magnetic resonance and biochemical experiments determined the C-terminal 30 residues of Pup to interact with PafA and Dop[3,21].

Considering the central role of Pup in the Pup-proteasome pathway it is of significant interest to understand the mechanism of its recognition by various components of the system. While our previous structural study gave an indication of the area where Pup might bind, it did not provide any structural information on Pup or its mode of binding to the ligase. However, this is of particular interest, since Pup is an intrinsically disordered protein and therefore the binding process is not a mere docking event, but involves the induced folding of Pup upon interaction with the ligase.

Here, we report the crystal structure of a complex between the minimal ligation-competent Pup fragment[21] with the ligase PafA at 2.8 Å resolution, which together with biochemical experiments provides the molecular framework for understanding the recognition of Pup by the pupylation enzymes.

To structurally characterize the interaction of the ligase PafA with Pup, a binary complex suitable for co-crystallization was generated. PafA crystals previously used for structure determination of the enzyme without Pup, featured an arrangement of PafA molecules precluding Pup-binding due to space constraints. To prevent formation of the same crystal form and to ensure an equimolar ratio of PafA to Pup in the crystal a fusion strategy was employed, where PafA from *Corynebacterium glutamicum* was C-terminally fused with Pup or N-terminally truncated fragments of Pup from the same organism. Crystals were obtained only with the shortest fragment tested, $PupE_{38\text{-}64}$. The reason is presumably that it displayed the least amount of flexibility while stabilizing the complex through formation of a dimer with the C-terminally fused $PupE_{38\text{-}64}$ reciprocally provided *in trans* to the Pup-binding groove of the opposing monomer (Supplementary Figure 1).

The structure of the PafA-Pup complex reveals that Pup binds to a conserved groove on PafA of about 40-50 Å in length that leads into the active site β-sheet cradle where ATP is bound (Figure 1a and 2a). The Pup:PafA interaction interface buries a large surface area of more than 1500 $Å^2$ (PISA PDB server).

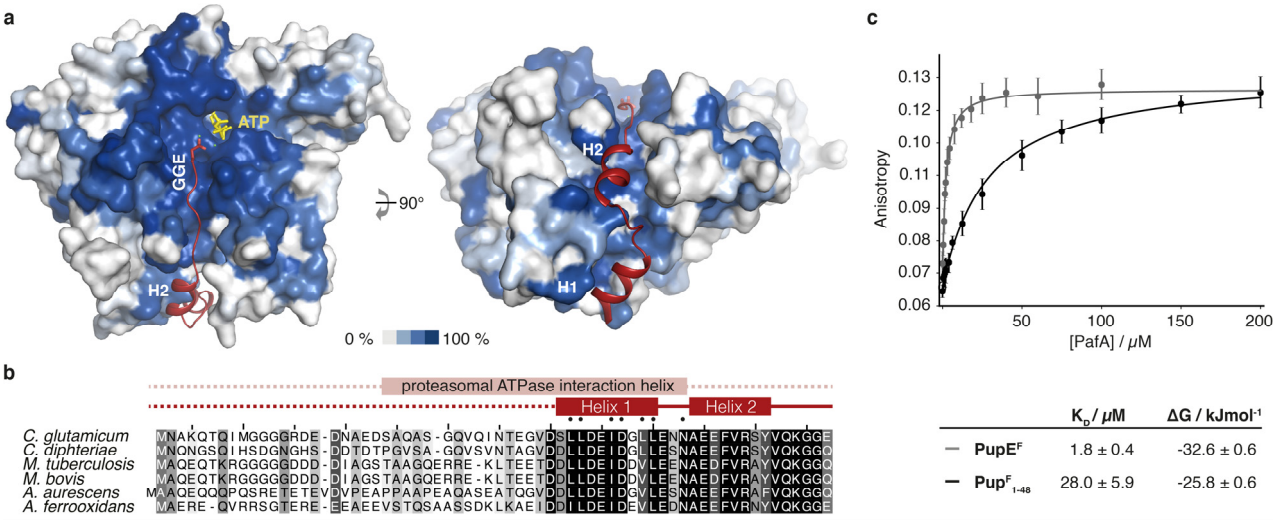

Figure 1. Pup binds to a conserved groove on PafA. (**a**) PafA acts as scaffold to induce folding of Pup (red) into two helices (H1, H2) connected by a short linker. The C-terminal glutamate and ATP (yellow) are shown in stick representation. The ligase is shown in surface representation colored according to conservation: from no conservation (white) to highly conserved (blue) (**b**) Alignment of Pups from different actinobacteria. The region involved in the interaction with the Pup ligase PafA (red) or the proteasomal ATPase Mpa/ARC (light red) is indicated. Residues involved in both interactions are marked with a dot. (**c**) Fluorescence anisotropy measurement with full length $PupE^F$ (grey) and C-terminally truncated $Pup^F{}_{1\text{-}48}$ (black). Error bars and uncertainties are given in terms of two standard errors.

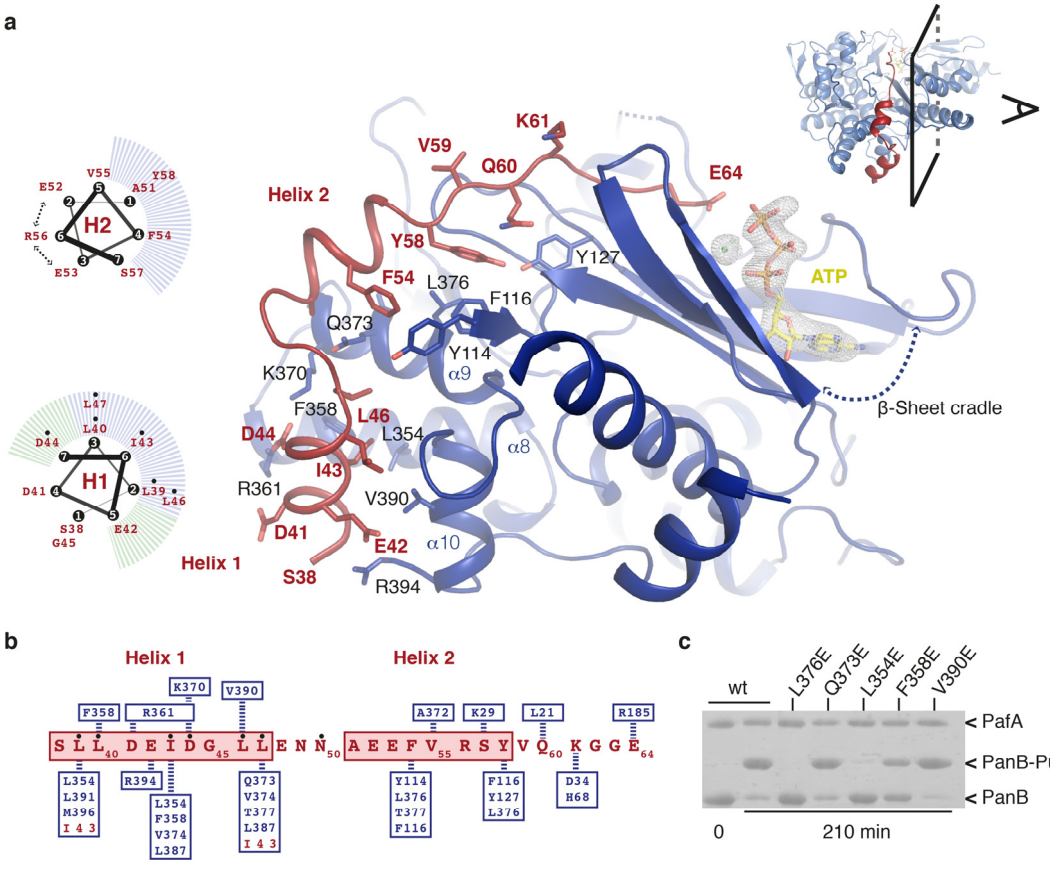

Figure 2. Interaction of the Pup ligase PafA with its ligands Pup, ATP and Mg^{2+}. (**a**) Slab view of PafA (blue) showing the molecular interaction with Pup (red) and ATP (yellow). Important residues are shown in stick representation. ATP and Mg^{2+} ions (green spheres) were modeled into the Fo-Fc difference density omit map (grey, contoured at 3 σ). A helical-wheel-representation (from N- to C-terminus) is shown next to H1 and H2. (**b**) Sequence of Pup (red) with H1 and H2 outlined as red boxes. PafA:Pup interactions are indicated with dashed lines. PafA residues are colored blue, Pup residues red. (**c**) Gel shift activity assay with PafA variants. Residues involved in the interaction with both Mpa and PafA are marked with a dot.

When binding to PafA, Pup undergoes a transition from the mostly disordered free state to forming two well-resolved helices (H1: S38-L47, H2: A51-Y58), orthogonal to one another and connected by a linker of three amino acids (E48-N50) (Figure 1a). Interestingly, the helix located further away from the active site (H1) is strictly required for the interaction with PafA/Dop, since $PupE_{38-64}$ is the shortest Pup fragment able to be conjugated to substrates by PafA[21] and $PupE_{44-64}^{AMC}$ showed no activity with Dop[22]. Pup-H1 completes formation of a four-helix bundle together with helices α8, α9 and α10 of PafA, anchoring Pup to the lower part of the Pup-binding groove (Figure 2a).

Upon binding, the 27 C-terminal Pup residues wrap around half of the PafA monomer. This arrangement could potentially serve to prevent an intra-molecular attack by a lysine in the flexible N-terminal region of Pup, which would be much faster than the inter-molecular attack by the substrate lysine and could compete with substrate tagging.

Pup binds into the PafA groove through a combination of hydrophobic interactions and salt bridges. A conserved hydrophobic pocket on PafA (L354, F358, V374, L387 and V390) responsible for interactions with H1, is bordered by positively charged residues (R357, R361, R394, K370) that complement negatively charged residues on Pup. The importance of this pocket, located more than 25 Å from the active site, in Pup binding is supported by PafA variants L354E and F358E, which retain no or only highly reduced activity, respectively (Figure 2c).

To further characterize binding of Pup to PafA, we carried out fluorescence anisotropy measurements (Figure 1c, Supplementary Figure 2). Full-length Pup binds to its ligase with low micromolar affinity (K_D = 1.8 ± 0.4 μM, Figure 1c, and [21]). To assess the contribution of the first helix to Pup binding, a Pup variant truncated C-terminally after the first helix (Pup^{F}_{1-48}) was used. The truncated variant showed reduced affinity (K_D = 28.0 ± 5.9 μM, Figure 1c). However, this still corresponds to a release of nearly 80 % of the total Gibbs free energy of binding assuming independence between H1 and H2. This implies that H1 provides the thermodynamic driving force in the PafA:Pup interaction. The second helix together with the five C-terminal residues is expected to be mostly involved in correct positioning of the glutamate in the active site. H2 contains two conserved aromatic residues (F54, Y58) that make stacking interactions with Y114, F116 and Y127 of PafA (Figure 2a). H2 is followed by the five C-terminal residues of Pup (VQKGGE) that are in an extended conformation. Pup-Q60 is completely buried and the C-terminal di-glycine motif is positioned by PafA-H68.

Taking into account the previously reported structure of a Pup-fragment in complex with the Mpa coiled-coil domains[20], our structure also reveals that Pup can adopt different folds depending on its interaction partner. In complex with Mpa, Pup-residues S21 to A51 form a helix (Figure 1b), while the C-terminal residues (E52 to Q64) remain disordered[20]. The structure adopted by Pup in complex with PafA on the other hand exhibits a helix-linker-helix conformation, despite a significant overlap in the interacting sequence regions on Pup involved in binding to Mpa and PafA, respectively. Based on the conservation of Dop's surface residues in the H1-binding region, it is likely that Dop interacts with Pup via a similar binding mode. This would imply that Dop and Mpa compete for Pup-modified proteins due to overlapping interaction interfaces, and that this competition might contribute to determining the fate of a pupylated substrate (degradation or depupylation).

ASSOCIATED CONTENT

Supporting Information

Supplementary methods. Supplementary Figure 1 to 3. Supplementary Table 1 with data collection and refinement statistics**.** Supplementary Table 2 with primers used in this study. Crystallographic data. This information is available free of charge via the internet at http://pubs.acs.org.

AUTHOR INFORMATION

Corresponding Author

* eilika@mol.biol.ethz.ch

ACKNOWLEDGMENT

We acknowledge the staff of X06SA at the Swiss Light Source for excellent support with data collection. We thank B. Blattmann and C. Stutz-Ducommun for help with initial screening. This work was supported by the Swiss National Science Foundation (SNSF), the National Center of Excellence in Research (NCCR) Structural Biology program of the SNSF and an ETH research grant.

REFERENCES

(1) Burns, K. E.; Darwin, K. H. *Cellular microbiology* **2010**, *12*, 424.
(2) Burns, K. E.; Liu, W. T.; Boshoff, H. I.; Dorrestein, P. C.; Barry, C. E., 3rd *J. Biol. Chem.* **2009**, *284*, 3069.
(3) Burns, K. E.; Pearce, M. J.; Darwin, K. H. *Journal of bacteriology* **2010**, *192*, 2933.
(4) Pearce, M. J.; Mintseris, J.; Ferreyra, J.; Gygi, S. P.; Darwin, K. H. *Science* **2008**, *322*, 1104.
(5) Striebel, F.; Imkamp, F.; Sutter, M.; Steiner, M.; Mamedov, A.; Weber-Ban, E. *Nat Struct Mol Biol* **2009**, *16*, 647.
(6) Barandun, J.; Delley, C. L.; Weber-Ban, E. *BMC biology* **2012**, *10*, 95.
(7) Striebel, F.; Hunkeler, M.; Summer, H.; Weber-Ban, E. *The EMBO journal* **2010**, *29*, 1262.
(8) Darwin, K. H.; Ehrt, S.; Gutierrez-Ramos, J. C.; Weich, N.; Nathan, C. F. *Science* **2003**, *302*, 1963.
(9) Gandotra, S.; Schnappinger, D.; Monteleone, M.; Hillen, W.; Ehrt, S. *Nature medicine* **2007**, *13*, 1515.
(10) Vijay-Kumar, S.; Bugg, C. E.; Cook, W. J. *Journal of molecular biology* **1987**, *194*, 531.
(11) Chen, X.; Solomon, W. C.; Kang, Y.; Cerda-Maira, F.; Darwin, K. H.; Walters, K. J. *Journal of molecular biology* **2009**, *392*, 208.
(12) Liao, S.; Shang, Q.; Zhang, X.; Zhang, J.; Xu, C.; Tu, X. *The Biochemical journal* **2009**, *422*, 207.
(13) Sutter, M.; Striebel, F.; Damberger, F. F.; Allain, F. H.; Weber-Ban, E. *FEBS letters* **2009**, *583*, 3151.
(14) Kerscher, O.; Felberbaum, R.; Hochstrasser, M. *Annual review of cell and developmental biology* **2006**, *22*, 159.
(15) Iyer, L. M.; Burroughs, A. M.; Aravind, L. *Biology direct* **2008**, *3*, 45.
(16) Guth, E.; Thommen, M.; Weber-Ban, E. *The Journal of biological chemistry* **2011**, *286*, 4412.
(17) Sutter, M.; Damberger, F. F.; Imkamp, F.; Allain, F. H.; Weber-Ban, E. *J Am Chem Soc* **2010**, *132*, 5610.
(18) Burns, K. E.; Cerda-Maira, F. A.; Wang, T.; Li, H.; Bishai, W. R.; Darwin, K. H. *Molecular cell* **2010**, *39*, 821.
(19) Imkamp, F.; Striebel, F.; Sutter, M.; Ozcelik, D.; Zimmermann, N.; Sander, P.; Weber-Ban, E. *EMBO Rep* **2010**, *11*, 791.
(20) Wang, T.; Darwin, K. H.; Li, H. *Nat Struct Mol Biol* **2010**, *17*, 1352.
(21) Ozcelik, D.; Barandun, J.; Schmitz, N.; Sutter, M.; Guth, E.; Damberger, F. F.; Allain, F. H.; Ban, N.; Weber-Ban, E. *Nature communications* **2012**, *3*, 1014.
(22) Merkx, R.; Burns, K. E.; Slobbe, P.; El Oualid, F.; El Atmioui, D.; Darwin, K. H.; Ovaa, H. *Chembiochem* **2012**, *13*, 2056.

Supplementary Information

Crystal structure of the complex between Prokaryotic Ubiquitin-like Protein Pup and its Ligase PafA

Jonas Barandun, Cyrille L. Delley, Nenad Ban and Eilika Weber-Ban*

ETH Zurich, Institute for Molecular Biology & Biophysics, CH-8093 Zurich, Switzerland

SUPPLEMENTARY METHODS

Cloning

All genes were obtained by PCR from *Corynebacterium glutamicum ATCC 13032* genomic DNA. All used primers are listed in Supplementary Table 2. To produce the PafA-linker-Pup_{38-64} constructs, we amplified *pafA* with primers P3/P4 and *pup* with primers P7/P8. The resulting PCR products were used as template in a second fusion PCR reaction performed with primers P3/P8. The final PCR product was cloned via AvrII and AflII into a modified pET24 vector (Novagen) containing a N-terminal His_6-tag followed by a TEV cleavage site. The modified pET24 vector was created by annealing and subcloning of the oligonucleotides P1 and P2 using restriction sites NdeI and SacI. The final construct consists of **NdeI**-His6-Tev-**AflII**-*pafA*$_{Cglu}$-**BamHI**-**NheI**-**KpnI**-*pup*$_{38-64}$*Q*-Stop-**AvrII**-**SacI**, resulting in the expression of the protein His_6-ENLYFQGLK-PafA-GSASGT-$PupQ_{38-64}$. Pup's C-terminal glutamate (Q64E) and the $PafA^{D64N}$ active site mutation were introduced by site directed mutagenesis according to the Stratagene QuikChange® protocol using primers P9/P10 and P11/P12. All other *pafA* mutants were generated using primers P13 to P20 and a previously used C-terminally His_6-tagged $PafA_{Cglu}$ construct as template[1]. The $PupE_{Cglu}$ construct was created by subcloning of a previously used pET-20-His_6-Thioredoxin-TEV-Pup_{Cglu}E into pET24 using restriction enzymes NdeI and SacI. The Q30C (P21/P22) and N49STOP (P23/P24) mutations were generated by site directed mutagenesis. All restriction enzymes used in this study were purchased from New England Biolabs.

Expression and purification of proteins

PafA wild type and all variants were purified as described[1]. The fusion constructs were expressed in *Escherichia coli* Rosetta (DE3) cells (Invitrogen). Expression was induced with 1 mM IPTG at 23 °C for 16 hours. All fusion constructs were purified by Ni-affinity chromatography (HiTrap IMAC HP, GE Healthcare) in 50 mM Tris, pH 7.5 (4 °C) 300 mM NaCl. After cleavage of the fusion protein with TEV-protease (Invitrogen), the histi-

dine tag and TEV-protease were removed by Ni-affinity chromatography. All proteins were further purified on a Superose 6 gel filtration column (66 ml) in 50 mM Tris, pH 7.5 (4 °C), 300 mM NaCl, 1 mM DTT and 20 mM $MgCl_2$ for activity assays or in 20 mM Tris, pH 7.5 (4 °C), 100 mM NaCl, 2 mM DTT and 5 mM $MgCl_2$ for crystallization.

Crystallization and crystal stabilization

PafA from *Corynebacterium glutamicum* ($PafA_{Cglu}$) was C-terminally fused to the $PupE_{38-64}$ fragment that was previously identified as the shortest fragment still able to be ligated to a substrate[1]. To abolish unspecific pupylation of *E. coli* proteins, an inactive variant of PafA was used to construct the fusion with ligation-competent Pup ($PafA^{D64N}PupE_{38-64}$).

Crystallization of the PafA-Pup fusion was performed in sitting drop vapor diffusion plates at a protein concentration of 10-20 mg ml^{-1} by mixing 1 µl of protein solution with 1 µl of mother liquor. Small crystals (20 * 20 * 50 µm) grew in 100 mM MES, pH 6.8, 150-200 mM Sodium Tartrate and 2-4 % PEG 4000 between day 10 and day 20 at 4 °C. Prior to flash-freezing, the small and fragile crystals were first stabilized for 5 days in 2 µl 100mM MES, pH 6.8, 100 mM Sodium Tartrate, 15 % PEG 4000 and then for 1h in cryo buffer (100 mM MES, 100 mM Sodium Tartrate, 15 % PEG 4000, 20 % PEG 400, 1 mM ATP, 5 mM $MgCl_2$).

Data collection, structure determination and refinement

Data were collected at beamline X06SA of the Swiss Light Source (PSI, Villigen, Switzerland) at an X-ray wavelength of 1 Å. Due to high radiation damage, the filter transmission had to be set to 10 % of the beam intensity. Data were indexed, integrated and scaled using X-ray detector software (XDS[2]). As input model for molecular replacement we used a $PafA_{Cglu}$ monomer (residue 1 to 51 from chain b and 52 to 478 from chain a) from the previously determined crystal structure of PafA (PDB 4B0T[1]). The model was built using COOT[3] and refined using phenix.refine[4].

The fusion protein crystallized in space group $P2_12_12_1$ and the crystals diffracted to 2.8 Å (Supplementary Table 1). The asymmetric unit contains two $PafA^{D64N}$-$PupE_{38-64}$ molecules arranged back to back with the C-terminally fused $PupE_{38-64}$ provided *in trans* to the Pup-binding groove of the opposing monomer (Supplementary Fig. 1a and b). The final electron density map showed continuous density for $PafA^{D64N}$ and $PupE_{38-64}$ except for two short loops (L170-S175, A196-S200) of $PafA^{D64N}$ and the linker region connecting $PafA^{D64N}$ with $PupE_{38-64}$. Although free, unbound Pup is unstructured and highly flexible[5-7], it is well resolved in the structure of the complex (Supplementary Fig. 1b and c). The difference density in the Pup-binding groove shows for both PafA monomers a continuous difference density although one of the two Pups is better resolved. The linker region (GSASGT) between PafA and Pup shows a tendency to adopt helical conformation, which extends the N-terminal region of Pup-H1. This extended H1 consisting of the artificial, flexible linker can be observed in one of the two monomers.

$PafA^{D64N}$-$PupE_{38-64}$ crystals where soaked with ATP and Mg^{2+} ions prior to freezing. The resulting difference density at the ATP binding position shows high occupancy in both monomers. Two magnesium ions can be observed. The first ion is located below ATP and is coordinated by residues of PafA (E16, Y62, E70) and coordinates the β- and γ-phosphates of ATP (Supplementary Fig. 3). A second magnesium ion is coordinated by E16, H130 and H221. Weak difference density located at the position where related GS bind glutamate/glutamine can be observed, and Pup's C-terminal glutamate can be modeled into this density, although with low occupancy. This might be due to the flexible di-glycine motif preceding E64 and agrees well with previous NMR measurements that show significant flexibility for the last three residues of Pup when bound to PafA[1].

Due to the presence of the native ligands (Pup, two Mg^{2+} ions and ATP) that stabilize the active conformation, several regions of the molecule surrounding the active site adopt a more biologically relevant conformation when compared to the previously solved structure of PafA from *C. glutamicum* in its free form[1] (PDB 4B0T) e.g. Y62 in strand β3 that positions a Mg^{2+} ion, or the orientation of the β3-β4-loop with the catalytically critical D64 that now points toward the glutamate-binding site.

Pup-conjugation assay

6 µM $PanB_{Mtb}$ and 1 µM $PafA_{Cglu}$ were incubated with 20 mM PupE in reaction buffer (50 mM Tris–HCl, pH 8 (23 °C), 300 mM NaCl, 20 mM $MgCl_2$) supplemented with 5 mM ATP at 23 °C as described[8]. The formation of a covalent PanB-Pup conjugate was analyzed by SDS–PAGE.

Fluorescence Anisotropy

The two cysteine-variants of Pup ($PupE^F$ or $Pup^F{}_{1\text{-}48}$) were labeled at Q30C with fluorescein-5-maleimide obtained from Life Technologies and purified on a Superdex75 gel filtration column (GE Healthcare). For fluorescence anisotropy measurements we incubated 0.5 µM of fluorescein labeled $PupE^F$ or $Pup^F{}_{1\text{-}48}$ with increasing concentrations of $PafA_{Cglu}$ (0 µM to 200 µM) at 23 °C in 50 mM Tris, pH 7.5, 300 mM NaCl, 10 % glycerol, 0.001 % Tween20. Measurements were performed on a PTI Quantamaster QM-7 spectrofluorometer in T-setup with excitation wavelength set to 492 nm and emission to 515 nm All measurements were performed at least as triplicates and data were fitted according to the following equation:

$$A = A_0 - (A_0 - A_\infty)\frac{(K_D + [PafA_0] + [Pup_0^F]) - \sqrt{(K_D + [PafA_0] + [Pup_0^F])^2 - 4[PafA_0][Pup_0^F]}}{2[Pup_0^F]}$$

A denotes anisotropy, A_0 and A_∞ the anisotropies of free and completely bound Pup^F, respectively. The pre-equilibria concentrations are given in $[Pup^F{}_0]$ and $[PafA_0]$ and the dissociation constant by K_D. A_0, A_∞ and K_D are the free parameters of the linear least square regression weighted by the inverse variance of the data points. Associated changes in Gibbs free energy were calculated according to:

$$\Delta_r G° = RTln(K_D)$$

Where $\Delta_r G°$ denotes the standard change of binding in Gibbs free energy, R is the gas constant, T the absolute temperature and $\ln(K_D)$ the natural logarithm of the molar dissociation constant.

SUPPLEMENTARY FIGURES

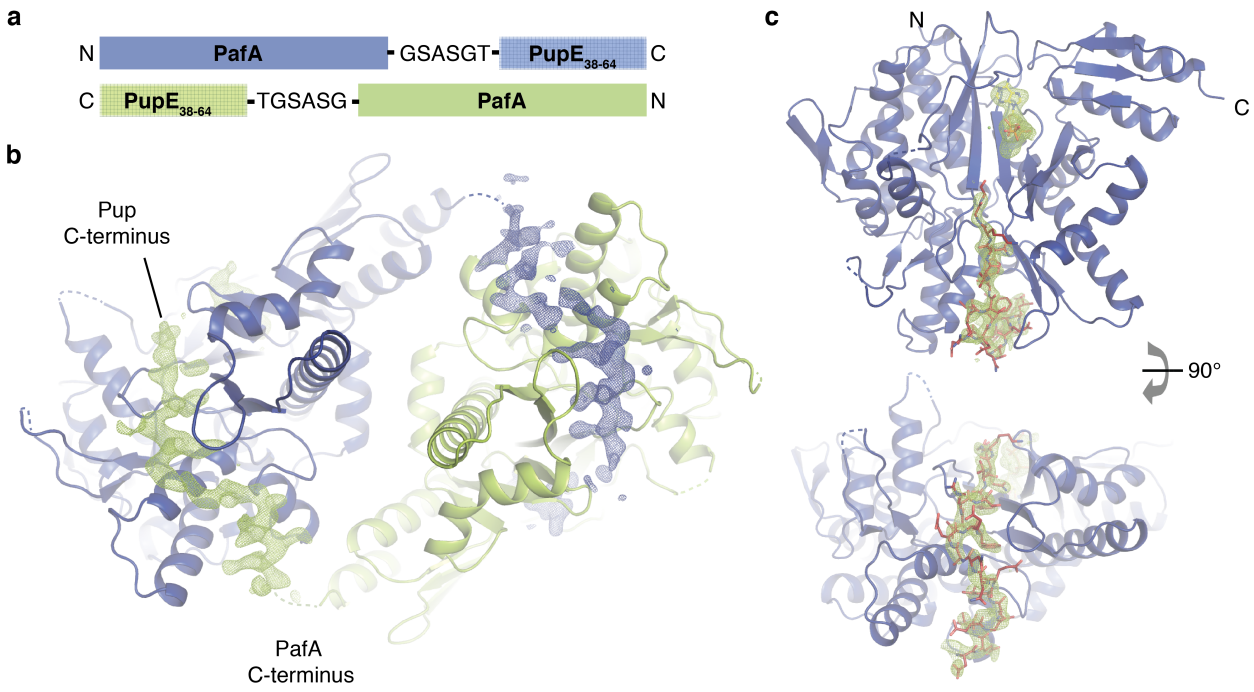

Supplementary Figure 1. $PafA^{D64N}PupE_{38-64}$ forms a dimer in the asymmetric unit. (**a**) Schematic representation of the PafA-Pup fusion construct and arrangement of the two protomers in the crystal. (**b**) Back-to-back arrangement of PafA (cartoon blue and green) in the asymmetric unit pointing the fused $PupE_{38-64}$ (Fo-Fc difference density, contoured at 2.7σ) into the Pup binding site of the second monomer. (**c**) Unbiased simulated annealing Fo-Fc difference density map generated using a model omitting all ligands (Pup, ATP, Mg^{2+}, H_2O).

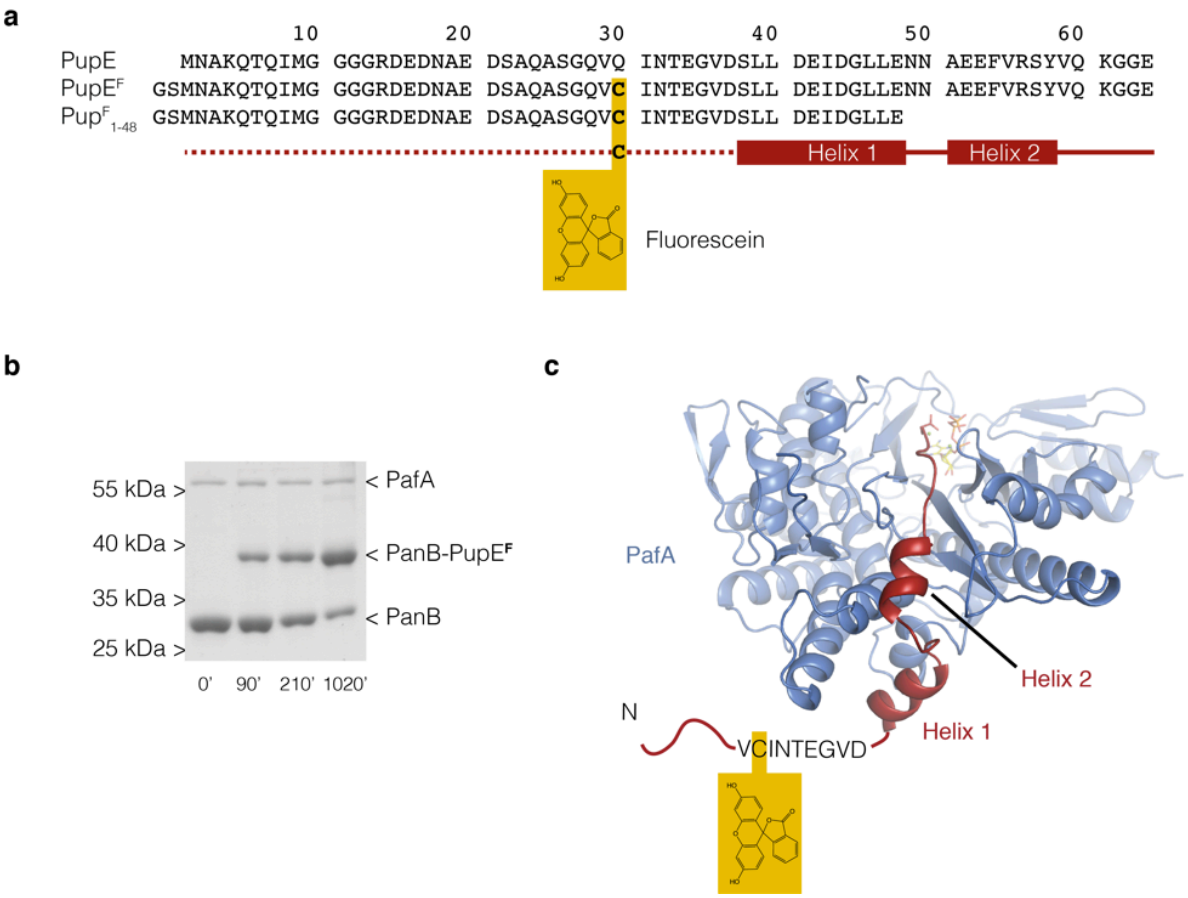

Supplementary Figure 2. Fluorescein-labeled Pup variant Q30C can be coupled to PanB. (**a**) Sequences of all used PupE constructs. Secondary structure elements are shown below the sequences (Helix 1, Helix 2). The mutation Q30C is highlighted yellow indicating the position of the fluorophore (fluorescein). (**b**) Gelshift assay monitoring pupylation of PanB (6 µM) with fluorescein-labeled Pup (18 µM) by PafA (0.5 µM). (**c**) PafA (blue) in complex with Pup (red) shows the location of the fluorescein-labeled cysteine in front of Helix 1.

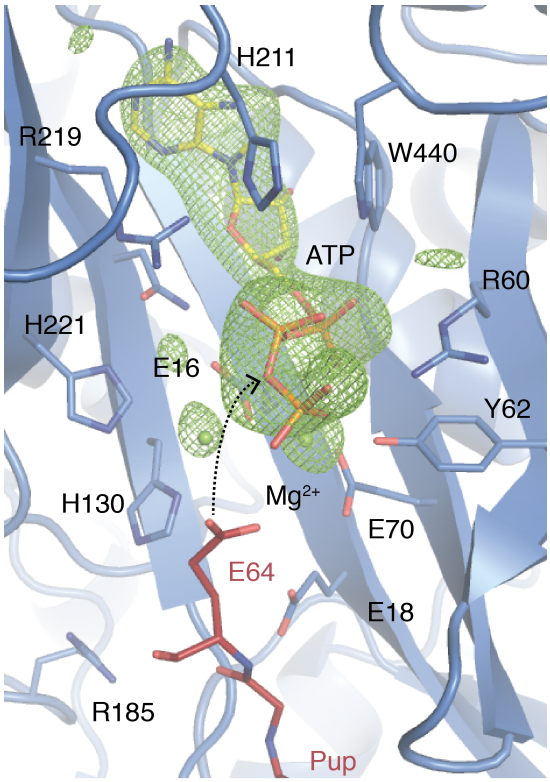

Supplementary Figure 3. The active site of PafA (blue). The C-terminal glutamate of Pup is shown in stick-representation (red). The unbiased simulated annealing Fo-Fc difference density map generated using a model omitting ATP, Mg^{2+} and H_2O is shown as green mesh (contoured at 3σ). ATP and Mg^{2+} (green spheres) are modeled into the difference density.

SUPPLEMENTARY TABLES

Supplementary Table 1. Data collection and refinement statistics.

	$Paf^{D64N}Pup27E$ ATP
Data collection	
Radiation source	SLS X06SA
Radiation wavelength (Å)	1.00
Space group	$P2_12_12_1$
Cell dimensions	
a, *b*, *c* (Å)[a]	63.84 84.02 215.11
Resolution (Å)	39-2.8
R_{merge} (%)	11.1 (67.1)
$\langle I \rangle / \langle \sigma(I) \rangle$	11.8 (2.44)
Completeness (%)	99.6 (99.8)
Redundancy	4.9
Refinement	
Resolution (Å)	2.8
No. reflections	29211
R_{work} / R_{free}	0.213/0.248
No. atoms	
Protein	7773
Ligand/ion	2 ATP 3 Mg^{2+}
Water	134
B-factors	
Protein	66.6
Nucleotide	68.4
Mg^{2+}	73.9
Water	55.8
RMSD	
Bond lengths (Å)	0.012
Bond angles (°)	1.118
PDB code	4bjr

Values in parentheses are for highest-resolution shell. [a] unit cell angles: α, β, γ = 90.0°, 90.0°, 90.0°

Supplementary Table 2. Primers used in this study.

Nr.	Constructs/PCR product	Primer	Sequence of PCR primer (5'-XX-3', restriction site: ***bold***)
P1	pET24-NdeI-H_6TEV-AflII-AvrII-SacI_MCS	fwd	***TAT G***CA CCA TCA CCA TCA CCA TGG CGA GAA TCT TTA TTT TCA GGG C***CT TAA G***AT ATA TAT AAT ATA TAT A***CC TAG GGA GCT***
P2	pET24-NdeI-H_6TEV-AflII-AvrII-SacI_MCS	rev	CCC TAG GTA TAT ATA TTA TAT ATA TCT TAA GGC CCT GAA AAT AAA GAT TCT CGC CAT GGT GAT GGT GAT GGT GC
P3	AflII-PafA$_{Cglu}$-GSASGT	PafA-fwd	GCT GGC TAT ***CTT AAG*** AGT ACC GTG GAA TCC GCA TTG ACC
P4	AflII-PafA$_{Cglu}$-GSASGT	PafA-rev	***GGT ACC GCT AGC GGA TCC*** ACT GCG ATA GCT TTC TGC ATG AAC
P7	GSASGT-Pup**Q**$_{38-64}$-AvrII	Pup$_{38-64}$-fwd	AGT ***GGA TCC GCT AGC GGT ACC*** AGC TTG CTG GAT GAA ATC GAC
P8	GSASGT-Pup**Q**$_{38-64}$-AvrII	Pup$_{38-64}$-rev	CAC GCC TAT ***CCT AGG*** TTA **CTG** GCC ACC CTT TTG TAC ATA
P9	Pup Q64E	fwd	TAT GTA CAA AAG GGT GGC GAA TAA ***CCT AGG*** GAG CTC CGT
P10	Pup Q64E	rev	ACG GAG CTC ***CCT AGG*** TTA TTC GCC ACC CTT TTG TAC ATA
P11	PafA$_{Cglu}$ D64N	fwd	GGT TCC CGC TTG TAT CTT GCC GTG GGT TCC CAC CCG GAG
P12	PafA$_{Cglu}$ D64N	rev	CTC CGG GTG GGA ACC CAC GGC AAG ATA CAA GCG GGA ACC
P13	PafA$_{Cglu}$ L354E	fwd	GTG ATC AAA AAG AAG GAA ATT GAT CGT TTC ATT
P14	PafA$_{Cglu}$ L354E	rev	AAT GAA ACG ATC AAT TTC CTT CTT TTT GAT CAC
P15	PafA$_{Cglu}$ F358E	fwd	AAG CTC ATT GAT CGT GAA ATT CAG CGC GGC AAC
P16	PafA$_{Cglu}$ F358E	rev	GTT GCC GCG CTG AAT TTC ACG ATC AAT GAG CTT
P17	PafA$_{Cglu}$ Q373E	fwd	GAT GAT CCA AAA CTT GCC GAA GTG GAC TTG ACT TAT CAC
P18	PafA$_{Cglu}$ Q373E	rev	GTG ATA AGT CAA GTC CAC TTC GGC AAG TTT TGG ATC ATC
P19	PafA$_{Cglu}$ V390E	fwd	AGA GGC CTA TTT AGC GAA CTG CAA AGC CGC GGC
P20	PafA$_{Cglu}$ V390E	rev	GCC GCG GCT TTG CAG TTC GCT AAA TAG GCC TCT
P21	Pup Q30C	fwd	CAG GCA TCT GGA CAG GTT TGC ATC AAC ACC GAA GGT GTG
P22	Pup Q30C	rev	CAC ACC TTC GGT GTT GAT GCA AAC CTG TCC AGA TGC CTG
P23	Pup N49*	fwd	ATC GAC GGA CTG TTG GAA TAA AAC GCC GAG GAA TTC GTT
P24	Pup N49*	rev	AAC GAA TTC CTC GGC GTT TTA TTC CAA CAG TCC GTC GAT

SUPPLEMENTARY REFERENCES

(1) Ozcelik, D.; Barandun, J.; Schmitz, N.; Sutter, M.; Guth, E.; Damberger, F. F.; Allain, F. H.; Ban, N.; Weber-Ban, E. *Nature communications* 2012, *3*, 1014.

(2) Kabsch, W. *Acta crystallographica. Section D, Biological crystallography* 2010, *66*, 125.

(3) Emsley, P.; Lohkamp, B.; Scott, W. G.; Cowtan, K. *Acta crystallographica. Section D, Biological crystallography* 2010, *66*, 486.

(4) Adams, P. D.; Afonine, P. V.; Bunkoczi, G.; Chen, V. B.; Echols, N.; Headd, J. J.; Hung, L. W.; Jain, S.; Kapral, G. J.; Grosse Kunstleve, R. W.; McCoy, A. J.; Moriarty, N. W.; Oeffner, R. D.; Read, R. J.; Richardson, D. C.; Richardson, J. S.; Terwilliger, T. C.; Zwart, P. H. *Methods* 2011, *55*, 94.

(5) Chen, X.; Solomon, W. C.; Kang, Y.; Cerda-Maira, F.; Darwin, K. H.; Walters, K. J. *Journal of molecular biology* 2009, *392*, 208.

(6) Liao, S.; Shang, Q.; Zhang, X.; Zhang, J.; Xu, C.; Tu, X. *The Biochemical journal* 2009, *422*, 207.

(7) Sutter, M.; Striebel, F.; Damberger, F. F.; Allain, F. H.; Weber-Ban, E. *FEBS letters* 2009, *583*, 3151.

(8) Striebel, F.; Imkamp, F.; Sutter, M.; Steiner, M.; Mamedov, A.; Weber-Ban, E. *Nat Struct Mol Biol* 2009, *16*, 647.